Available online at www.sciencedirect.com
ScienceDirect
Ultramicroscopy 107 (2007) 934–942
ultramicroscopy
www.elsevier.com/locate/ultramic

Comparison of the indentation and elasticity of *E. coli* and its spheroplasts by AFM

C.J. Sullivan[a,c], S. Venkataraman[c], S.T. Retterer[c], D.P. Allison[a,b,c,d], M.J. Doktycz[a,c,*]

[a]*Genome Science and Technology, The University of Tennessee, Knoxville, TN 37932, USA*
[b]*Department of Biochemistry & Cellular & Molecular Biology, The University of Tennessee, Knoxville, TN 37932, USA*
[c]*Biosciences Division, Oak Ridge National Laboratory, Oak Ridge, TN 37831-6123, USA*
[d]*Agilent Technologies, Tempe, AZ 85282, USA*

Abstract

Atomic force microscopy (AFM) provides a unique opportunity to study live individual bacteria at the nanometer scale. In addition to providing accurate morphological information, AFM can be exploited to investigate membrane protein localization and molecular interactions on the surface of living cells. A prerequisite for these studies is the development of robust procedures for sample preparation. While such procedures are established for intact bacteria, they are only beginning to emerge for bacterial spheroplasts. Spheroplasts are useful research models for studying mechanosensitive ion channels, membrane transport, lipopolysaccharide translocation, solute uptake, and the effects of antimicrobial agents on membranes. Furthermore, given the similarities between spheroplasts and cell wall-deficient (CWD) forms of pathogenic bacteria, spheroplast research could be relevant in biomedical research. In this paper, a new technique for immobilizing spheroplasts on mica pretreated with aminopropyltriethoxysilane (APTES) and glutaraldehyde is described. Using this mounting technique, the indentation and cell elasticity of glutaraldehyde-fixed and untreated spheroplasts of *E. coli* in liquid were measured. These values are compared to those of intact *E. coli*. Untreated spheroplasts were found to be much softer than the intact cells and the silicon nitride cantilevers used in this study.
© 2007 Elsevier B.V. All rights reserved.

Keywords: Atomic force microscopy; Bacteria; E. coli; Spheroplast; Elasticity

1. Introduction and significance

Gram-negative bacteria have a cell wall, which includes the peptidoglycan, a gel-like periplasm, and an outer membrane with appendages such as fimbriae, pili, and flagella. Beneath the peptidoglycan, which determines the shape and rigidity of the bacteria, is the cytoplasmic membrane. Transporters, channels and other proteins whose function is to selectively exchange materials between the cell and its environment are localized within this membrane [1] (Fig. 1). Removal of the cell wall allows access to the cytoplasmic membrane and results in the formation of spherical, osmotically sensitive cells called spheroplasts [2,3]. Spheroplasts are viable and can be grown in broth where they retain a uniformly spherical shape. This uniformity is lost when the spheroplasts are grown on soft agar, a characteristic attributed to differences in local stresses provided by the agar [4,5]. Nevertheless, specialized growth conditions have been formulated for their long-term propagation *in vitro* [6–8]. Spheroplasts of various bacteria have proven to be useful research models to study mechanosensitive ion channels, lipopolysaccharide translocation, solute uptake, and the effects of antimicrobial agents [9–13].

Clinical and histological studies have revealed that bacteria without cell walls, known as cell wall-deficient (CWD) forms, are present in human diseases including Lyme disease, Crohn's disease, endocarditis, acute coronary syndromes, sarcoidosis, osteomyelitis, arthritis, inflammatory bowel syndrome, and meningitis [14–16]. Complications in bone marrow transplants and disease treatment as a result of antibiotic resistance have also been

*Corresponding author. Biosciences Division, Oak Ridge National Laboratory, Oak Ridge, TN 37831-6123, USA.
E-mail address: doktyczmj@ornl.gov (M.J. Doktycz).

0304-3991/$ - see front matter © 2007 Elsevier B.V. All rights reserved.
doi:10.1016/j.ultramic.2007.04.017

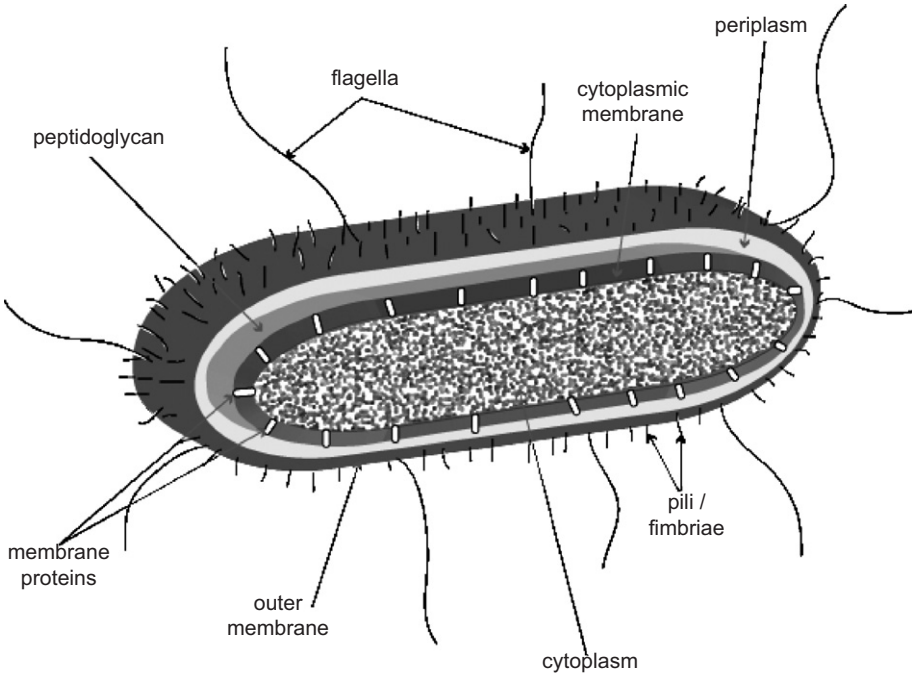

Fig. 1. The cellular structure of *E. coli*. Removal of the cell wall results in osmotically sensitive spheroplasts.

associated with CWD bacteria [15]. Interestingly, CWD have also been used as plant biocontrol agents as they can form symbiotic relationships with plants [6]. The application of genetic techniques to the study of CWD and spheroplasts is limited because they are genetically identical to their intact bacterial counterparts. Electron microscopy (EM) has played a significant role in characterizing these organisms [2,8,15–18]. Although high-resolution imaging is possible with EM, the requirements for fixation and staining of samples for image contrast severely limits the study of living organisms. Atomic force microscopy (AFM) would be an attractive technique for studying these organisms because they could be maintained and imaged in biocompatible conditions. Moreover, AFM is capable of simultaneously achieving nanometer spatial resolution and piconewton force detection allowing for detailed studies of cell surface morphology and monitoring of cell–tip interactions. This capability has been used to measure cell elastic and structural properties, identify specific molecules in the membrane of living cells and to measure binding affinities at the single molecule level [19–26]. It is expected that the approaches described in this paper for imaging spheroplasts by AFM would also be relevant to investigations of other cell types including CWD forms.

Imaging bacterial cells by AFM requires that the cells are stably immobilized, so that they are not displaced by forces generated by the tip during scanning. Immobilization procedures are established for intact bacteria and have facilitated investigations on elasticity, adhesion, surface structure, and swarming behavior [27–30]. A simple, effective, and general immobilization strategy for both gram-negative and gram-positive bacteria is to briefly incubate a bacterial suspension on a gelatin-coated mica surface [31,32]. Immobilization on the gelatin-coated mica is sufficiently robust for intermittent and contact mode imaging techniques and it is used in the current study for the immobilization of intact bacteria. Adhesion molecules, present on the exposed surfaces of bacteria, likely account for their immobilization on gelatin [33,34]. Spheroplasts and CWD require immobilization techniques different from intact bacteria and have yet to become the subject of extensive AFM investigations. While procedures for making spheroplasts have been established for decades, immobilizing them for study has only recently been reported [35]. In this paper, we describe a new immobilization technique for spheroplasts using aminopropyltriethoxysilane (APTES) and glutaraldehyde-treated mica, which allows stable imaging of the cells. Images of immobilized spheroplasts are presented as well as results from indentation and elasticity measurements on intact *E. coli*, glutaraldehyde-fixed spheroplasts and untreated spheroplasts of *E. coli*.

2. Materials and methods

2.1. Cell cultures

Cultures of *E. coli* in Luria Broth (LB) supplemented with 100 μg/ml ampicillin were grown overnight at 37 °C in a shaking incubator. A fresh culture was inoculated from the overnight culture on the morning of experimentation and returned to the incubator shaker for 5 h to insure that the cultures were in logarithmic phase when harvested.

2.2. Spheroplasting

The spheroplasting procedure used was an adaptation of the one published by Birdsell and Cota-Robles [2]. Briefly, 1 ml of the fresh logarithmic phase *E. coli* LB broth culture was collected by centrifugation and washed in 1 ml 0.01 M Tris–HCl buffer, pH 8.0 (TB). The cells were pelleted by centrifugation at 4.5 rcf (relative centrifugal force) and resuspended in 500 μl of a TB supplemented with 0.5 M sucrose (TBS1) to induce plasmolysis. After 20 min in a 37 °C incubator shaker, lysozyme (Sigma, St. Louis, MO) was added to the cell suspension at a final concentration of 50 μg/ml. After 20 min incubation in the incubator shaker, the suspension was diluted 1:1 with TB and EDTA was added to a final concentration of 10 mM. The suspension was returned to the 37 °C incubator shaker for an additional 30 min. After this incubation, transition of the rod-shaped bacteria into spheres was confirmed by light microscopy. The reaction was stopped by pelleting the cells at 0.5 rcf for 25 min. The spheroplasts were then washed in 1 ml TB with 0.25 M sucrose and 10 mM $MgSO_4$ (TBS2), pelleted at 0.5 rcf for 20 min and resuspended in 100 μl TBS2.

2.3. Mica preparation

2.3.1. APTES/Glut mica

The APTES/Glut mica was prepared according to a published procedure [36]. Briefly, the tops of two 1.5 ml tubes were cut and placed (open end up) in the bottom of a dessicator. The dessicator was purged with argon for 2 min. Freshly cleaved rectangles (22 × 30 mm) of cut mica were placed into the dessicator. To one top, 30 μl of APTES (99%; Sigma-Aldrich, St. Louis, MO) was added and 10 μl *N*,*N*-diisopropylethylamine (Sigma-Aldrich) was added to the other top. The dessicator was purged for 2 min and then sealed for 2.5 h. After this time, the two tops were removed and the dessicator purged for 2 min. The mica was removed and stored for later use in a sealed dessicator. Prior to immobilizing spheroplasts on the mica, 100 μl of 2.5% glutaraldehyde was added for 20 min, rinsed vigorously in a stream of nanopure-deionized water, dried under a stream of dry nitrogen and placed in a covered dish until used.

2.3.2. Gelatin-treated mica

A gelatin solution was prepared by dissolving 0.5 g gelatin (Sigma #G6144) in 100 ml of nanopure distilled water at 90 °C and cooled to 60 °C prior to vertically dipping several 22 × 30 mm rectangular, freshly cleaved mica surfaces into the solution. The gelatin-coated mica surfaces were supported on edge on a paper towel and then air dried overnight [27,31].

2.4. Immobilization of cells

2.4.1. Spheroplasts

A 100 μl aliquot of the spheroplast suspension was added to the APTES/Glut-prepared mica surface. After 1 h, the sample was rinsed in a stream of TBS2, placed in the AFM and imaged in the same buffer. Fixed spheroplasts were prepared likewise except after the 1 h incubation period on APTES/Glut mica, 100 μl of 0.5% glutaraldehyde was added to the immobilized spheroplasts for 20 min and rinsed in TBS2 prior to being imaged in the same buffer.

2.4.2. Intact bacteria

A 1 ml aliquot of a logarithmic culture of *E. coli* bacteria was pelleted by centrifugation, washed in the same volume of deionized water, pelleted again and resuspended in 500 μl of deionized water. Twenty microliters of this cell suspension was applied onto a gelatin-treated mica surface. The sample was allowed to stand for 10 min before it was rinsed in deionized water and imaged in the liquid cell of the AFM.

2.5. AFM

Samples were placed in the liquid cell of a PicoPlus atomic force microscope (Agilent Technologies, Tempe, AZ) and imaged using a 100 μm scanning head. The instrument was operated in MAC Mode® at 256 or 512 pixels per line scan at speeds ranging from 0.6 to 2 Hz.Cells were imaged using Type IVe and IVc silicon nitride cantilevers (MAClevers™, Agilent Technologies, Tempe, AZ) with nominal spring constants of 0.1 and 0.01 nN/nm, respectively. The resonant frequencies of the type IVe and IVc cantilevers in air are 38 and 7 kHz, respectively. Imaging in liquid was required for the experiments in this report because the spheroplasts are osmotically sensitive and must be maintained in a sucrose buffer to prevent lysis. Because the first harmonic of the type IVc cantilever in liquid was unreliable, the second harmonic, having a resonant frequency of approximately 6.5 kHz in liquid, was used. All of the images presented are first-order flattened.

2.6. Force curve acquisition in buffer

From a low-resolution MAC Mode® scan of a surface containing either intact bacteria or spheroplasts, an area of interest containing isolated cells was identified. This area was scanned at higher resolution and a single isolated bacterium of interest was identified within the scanned area. After recording this scan, the cursor was placed in the center of the identified bacterium and force curves were generated using a sweep duration of 0.2 s. After placing the cursor over the sample and allowing five force curves to be taken to stabilize the instrument, approximately 20 measurements were recorded. The cursor was then relocated to a region outside the perimeter of the cell on the substrate where at least six control force curves were similarly obtained. A subsequent image was generated to confirm that the condition and location of the cell of interest had not been changed by the force curve measurements.

2.7. Cantilever spring constant determination

Prior to measuring the elasticity of a sample, force curves were generated in contact mode from six 50 μm approaches to mica in air. The sweep duration of the force curves was 0.5 s. After each approach, the slope in the contact region from the fifth curve was recorded. The inverse of this slope is the conversion coefficient, which was entered into 'Thermal K', a program that interfaces with the imaging software to calculate the spring constant of a cantilever by the thermal method [37–39]. The mean of these six spring constants was called S1. After imaging a sample, six additional approaches to the surface in air were made. Force curves were generated for each approach and spring constants were again determined as described above. The mean of these spring constants was called S2. The average of S1 and S2 was used in the calculations as the spring constant of the cantilever.

2.8. Force curve analysis

A Matlab-based automatic algorithm was developed to analyze force distance curves in order to identify the approach region, obtain the slope in the region of constant compliance; identify the boundaries between regions; and to calculate the indentation values. An average of 20 force curves collected from each sample was plotted and the instantaneous slopes at each data point were calculated. The mean value of the last 20 points in the approach curve was calculated to be the slope over the constant compliance region. A line was drawn by using this slope and the median point over the sample space was used for determining the slope. Another line to mark the base of the curve was drawn by using a slope of zero and the first data point in the approach curve. In order to identify the end of the nonindentation region and the beginning of the constant compliance region, the data points from the shifted curve were fit to the two lines (base and slope, respectively) and a threshold (0.05) was set on the values obtained. Ideally, when the points fit the line, the value should be equal to zero and when it is greater than 0.05, we identified the point to be on the boundary. This threshold was user-defined and could be changed to suit the requirements. These two regions were then defined as well as the value of slope in the constant compliance region. In order to find the indentation, a reference control curve was

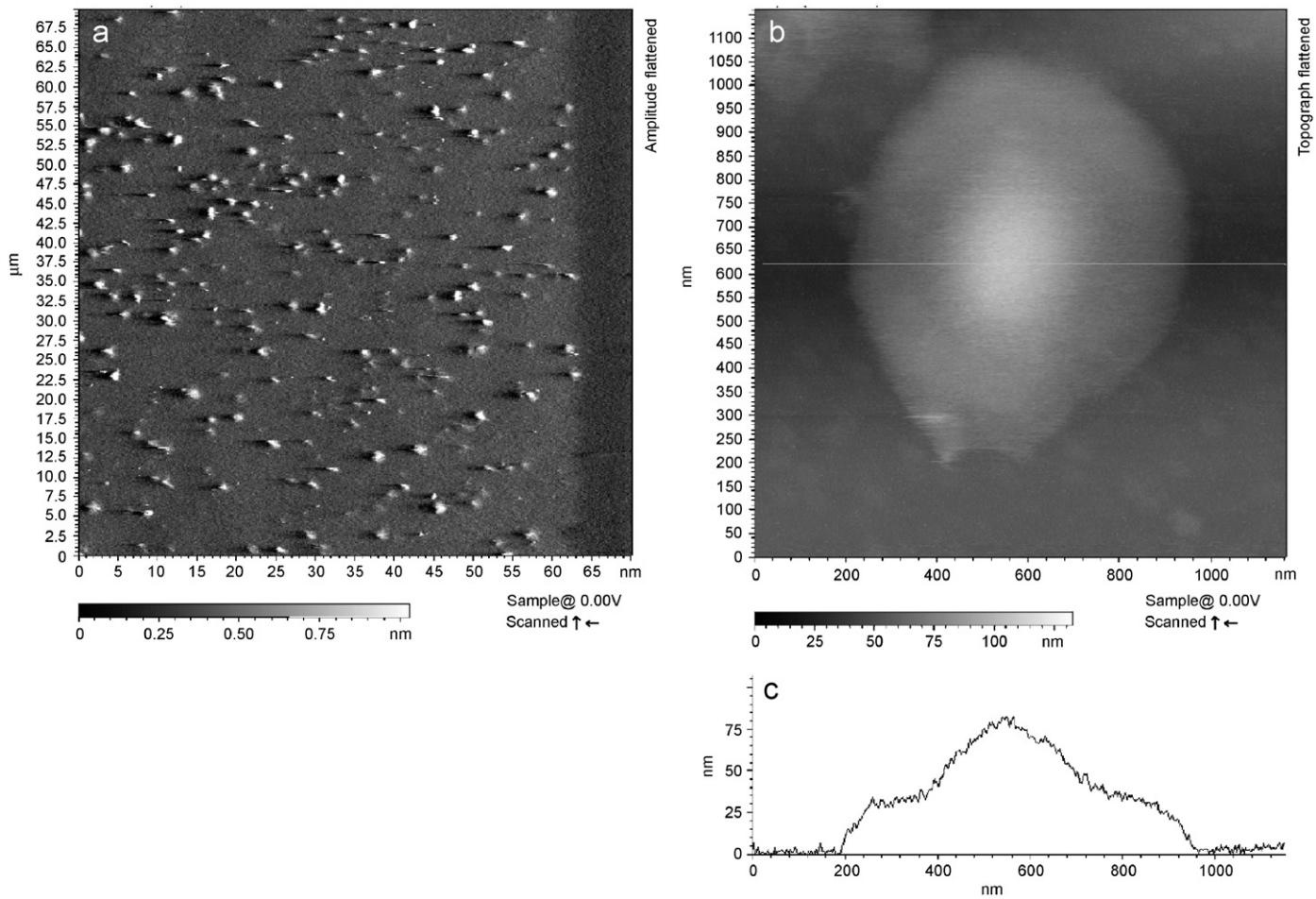

Fig. 2. Spheroplasts immobilized on APTES and glutaraldehyde-treated mica. MAC Mode® images taken with a silicon nitride cantilever having a nominal spring constant of 0.1 nN/nm: (a) 70 μm scan; (b) individual spheroplast; and (c) cross-section measurement of topograph image showing height.

obtained on the sample substrate. This curve was plotted with the force curves from the specimen.

3. Results and discussion

3.1. Spheroplast immobilization and morphology

The adhesion proteins believed to be responsible for immobilizing intact bacteria on gelatin are likely absent in spheroplasts upon removal of the cell wall, making gelatin-coated mica an unsuitable substrate for their immobilization [35]. Spherical yeast cells have been successfully trapped in isoporous membranes and subsequently imaged by AFM [20,40]. However, our attempts to immobilize spheroplasts this way have been unsuccessful, possibly because the rigid cell wall is absent and the flexible cell membrane allows the spheroplast to compress and pass through the filter. This idea is supported by the finding that CWD forms are able to penetrate filters having only 220 nm pores [16]. In view of these observations, alternate immobilization strategies must be developed specifically for bacteria that do not present surface molecules compatible with gelatin binding. In an earlier paper, we described an immobilization method where spheroplasts were mixed with warm gelatin on a mica surface [35]. It was demonstrated through confocal microscopy that using this technique results in some of the spheroplasts becoming embedded in the gelatin to various depths. It is also possible that a thin layer of gelatin covers the spheroplasts preventing direct contact between the tip and the cell. Furthermore, the possibility that the temperature of the gelatin affects the characteristics and integrity of the membrane cannot be eliminated. Therefore, a goal of the current study was to find an alternative immobilization technique that allows for rapid, facile mounting of cells and increased accessibility to the cantilever.

Glutaraldehyde is one of several cross-linking agents used in light, electron, and atomic force microscopies. It is a small molecule able to cross-link the free nitrogens of the amino acids of proteins with the aldehyde groups on both ends of the glutaraldehyde polymer [41]. Wang et al. reported that mica pretreated with aminopropyltriethox-

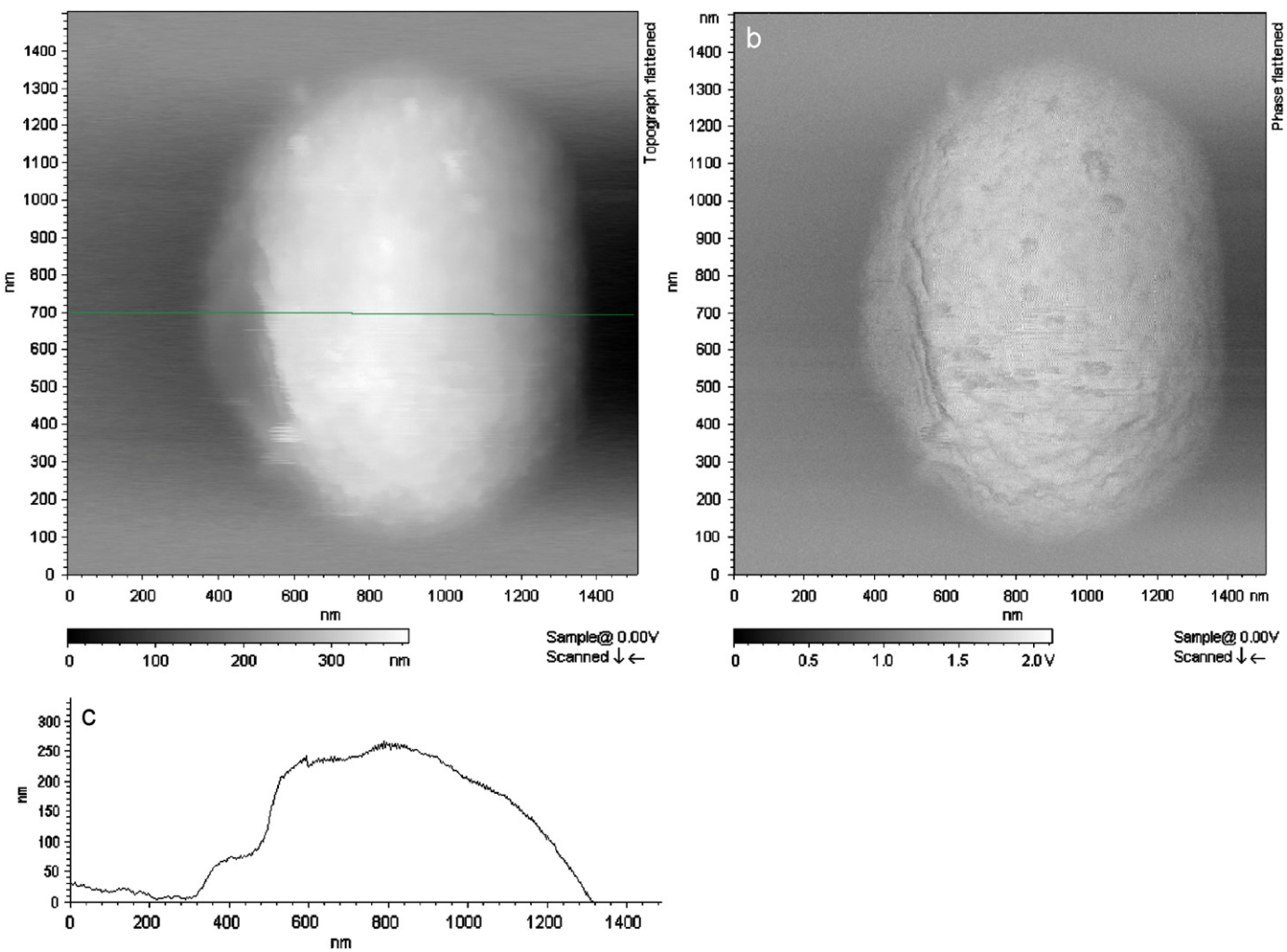

Fig. 3. MAC Mode® images of a 0.5% glutaraldehyde-fixed spheroplast acquired using a silicon nitride cantilever having a nominal spring constant of 0.1 nN/nm: (a) topograph image; (b) phase image; and (c) cross-section measurement of topograph image.

ysilane and glutaraldehyde (APTES/Glut) was an effective substrate for immobilizing and imaging chromatin using AFM [36]. The immobilization of chromatin was believed to result from interactions between proteins on the chromatin and the treated substrate. Adapting this procedure, an aliquot of a spheroplast suspension was applied to APTES/Glut-treated mica. Conceivably, only the surface of the spheroplast in contact with the mica surface is affected by the immobilization, leaving the exposed surface both in its native state and accessible to the tip. After incubation and washing, the spheroplasts were imaged by MAC Mode® AFM in buffer using a silicon nitride cantilever having a nominal spring constant of 0.1 nN/nm. The results are shown in Fig. 2. Measurements taken from individual spheroplasts immobilized this way reveal that the lateral diameters of the cells are approximately 1 μm, similar to measurements determined from EM images of thin sections [2]. Height measurements of approximately 100 nm, however, are considerably less than the diameter. Despite using MAC Mode®, an intermittent contact mode designed to minimize the vertical force applied during imaging, it is likely that the apparent compression of the spheroplast is caused by forces exerted by the tip.

Previous reports concluded that fixation of mammalian cells with glutaraldehyde increased the cellular elastic modulus significantly [42,43]. Since the exposed cytoplasmic membrane of spheroplasts is similar to the cellular membrane of mammalian cells, we conducted experiments to determine whether fixation of spheroplasts would also result in increased membrane rigidity. This was accomplished by treating the spheroplasts with 0.5% glutaraldehyde after they had been immobilized on APTES/Glut-treated mica. When these fixed spheroplasts were imaged by AFM in MAC Mode® with a silicon nitride cantilever having a spring constant of 0.1 nN/nm, the diameters of the fixed spheroplasts were similar to the untreated spheroplasts (Fig. 3). However, the height measurements were increased from 100 nm to around 250 nm. Nevertheless, the increased height measurements of the fixed spheroplasts compared to the unfixed spheroplasts were still considerably less than the diameters, raising the possibility that the glutaraldehyde-fixed spheroplasts were also being compressed by the AFM tip but to a lesser degree than unfixed spheroplasts.

To determine whether the reduced height was a consequence of the tip used for imaging or inherent to the spheroplasts, the experiment was repeated on untreated spheroplasts with the softer silicon nitride cantilever having a nominal spring constant of 0.01 nN/nm (Fig. 4). The resonant frequency of the first harmonic of this cantilever was very low and found to be unstable in liquid; therefore the second harmonic was used instead. Following this change to the softer cantilever (0.01 nN/nm), the height increased to 300–400 nm, as opposed to the 100 nm height found when imaging with the stiffer cantilever. These results further supported the notion that compression of the spheroplast occurred during imaging and was caused by excessive cantilever force. Untreated spheroplasts were also imaged in contact mode using the softer (0.01 nN/nm)

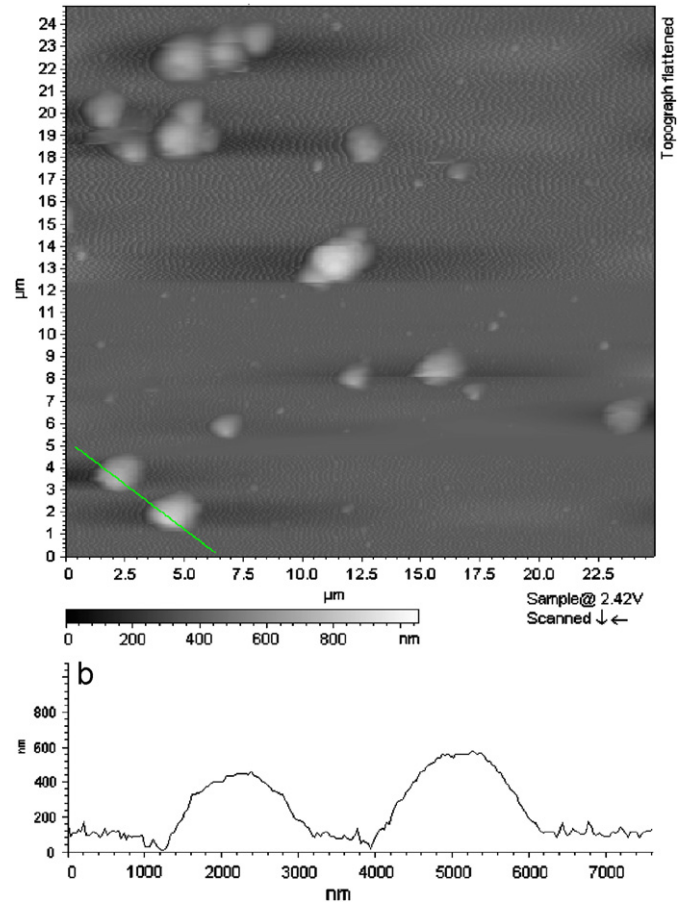

Fig. 4. Images of untreated spheroplasts acquired using a silicon nitride cantilever with a nominal spring constant of 0.01 nN/nm: (a) 25 μm scan taken in MAC Mode® and (b) cross-section measurement of the two spheroplasts identified in (a).

cantilever. The spheroplasts conformed to the shape of the tip and resulted in an image of the tip (data not shown). It is important to note that intermittent contact imaging, which applies a lower force, was required to prevent these tip artifacts. The APTES/Glut substrate stably immobilized the cells, as repeated contact mode imaging did not remove the cells. However, the spheroplasts were severely deformed and often punctured by the tip. Contact mode imaging of normal intact bacteria does not result in similar distortions nor were differences in height measurements noted between those taken with either of the cantilevers.

3.2. Indentation and elasticity measurements

Force distance curves record vertical cantilever deflection as the vertical piezo moves the AFM tip toward the surface, makes contact with the surface, and is retracted from the surface. These curves can be used to measure surface indentation and elasticity. To facilitate this application, force distance curves generated on a relatively hard surface such as mica are used to convert voltage into tip displacement in nanometers. When measuring the spring constant of a bacterium, two springs are present in

series (the bacterium and the cantilever). In this case, the cantilever deflection occurs over a greater distance as soft samples exhibit a gradual change in deflection initially. The spring constant of the bacterium (k_b) can be calculated using the equation $k_b = k_c s/(1-s)$, where k_c is the spring constant of the cantilever and s is the slope from a force curve taken on the bacterium [44]. The nominal spring constant, given by the manufacturer, of the softer cantilever is 0.01 nN/nm. However, in order to improve the accuracy of the spring constant calculations for bacteria and spheroplasts, we used the thermal method to directly measure the spring constants (k_c) of the cantilevers used in the following experiments. The spring constants of the cantilevers used on the intact bacteria, fixed spheroplasts and untreated spheroplasts were determined to be 0.0343, 0.0349 and 0.0519 nN/nm, respectively. The magnetic coating, which is added after the cantilever is manufactured, likely contributes to the difference in the spring constants over the nominal value reported by the manufacturer. Approach force distance curves were

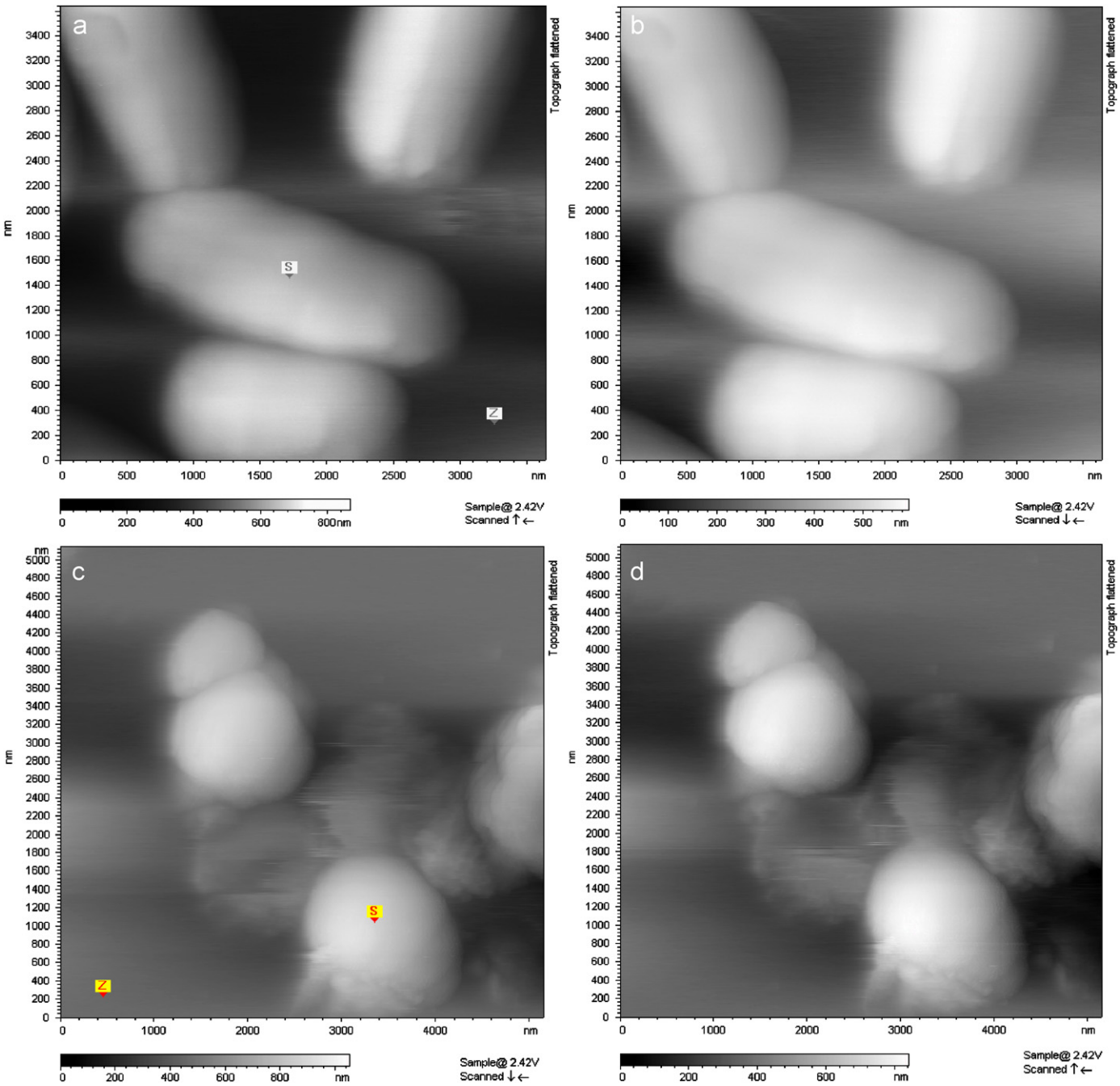

Fig. 5. (a–d) Topograph images taken in MAC Mode®. (a, b) Intact bacteria. (c, d) Fixed spheroplasts. (a, c) Locations where force distance curves were generated within the perimeter of the bacteria and on the substrate are represented by s and z, respectively. (b, d) Subsequent images were generated after force distance curves to verify the condition and location of the measured bacteria.

collected from selected locations on the surface of intact bacteria, fixed spheroplasts, and untreated spheroplasts. Approach force distance curves were also collected from nearby regions of the substrate surface for comparison. A subsequent image was generated to assess the condition and location of the measured cell (Fig. 5). For each data set, approximately 20 force distance curves were generated within the perimeter of the cell of interest. At least six force curves were generated at a location outside the cell on the substrate. The control force distance curves on the gelatin-treated mica were comparable to controls on APTES/Glut-treated mica suggesting that any difference between the substrates is negligible for this analysis.

To extract information about indentation from the force distance curves, a computer algorithm was developed to automatically divide the curves into regions. Similar analyses have been described by Li and Logan [45]. Relevant to this paper are the regions before sample contact and during constant compliance. Upon approach, the tip is too far away from the sample to be deflected; therefore the slope of the force curve before contact is zero. This region provides a base line and is set to zero cantilever deflection. Upon hard sample contact, the tip deflects. However, with soft samples, such as the cells measured here, the tip begins to indent the sample upon contact. This indentation causes the slope of the force distance curve to change continuously until the slope becomes constant in the constant compliance region.

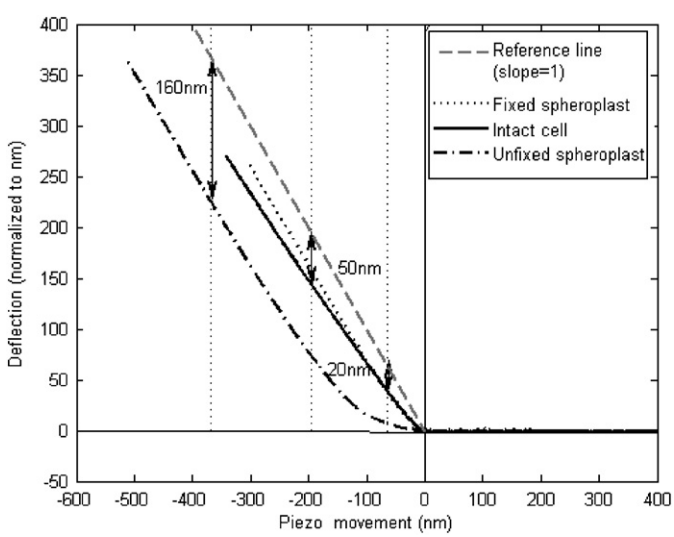

Fig. 6. Graph of composite force distance curves for the intact cell, spheroplasted cell, and fixed spheroplast. The dotted vertical lines indicate the start of the constant compliance regions for the three cell types. The indentation values for the three cell types are indicated.

To estimate indentation, control (hard surface) and experimental (cell surface) curves were plotted together. Indentation is defined as the difference between the two curves at the start of the constant compliance region (Fig. 6 and Table 1). The indentation for the intact bacterium is 50 nm, similar to values reported previously [44,45]. The least amount of indentation, 20 nm, occurred on the fixed spheroplast due to the stiffening of the membrane caused by the glutaraldehyde cross-linking. The 160 nm indentation of the untreated spheroplast is noteworthy because it represents a significant fraction of the total height of the spheroplast. Curvilinear regions exist in the force distance curves as a result of interactions between the tip and the bacterial surface. The curve is protracted in the case of the untreated spheroplasts because of its tendency to deform. Reaching the quasi-equilibrium represented by the linear region of the curve is thus delayed. While qualitative observations can be made, quantitative assertions about this region are complicated by the uncertain point of contact. Therefore, the degree of indentation is difficult to determine precisely. Moreover, it is impossible to know whether deflection occurs at the instant of contact or after significant indentation has occurred. If the latter is true, then the indentation for the untreated spheroplast is underestimated. This possibility is less of a concern in the intact bacteria because indentation is limited by the rigid peptidoglycan.

From the force curves generated with the softer cantilevers, slopes for intact *E. coli*, fixed and untreated spheroplasts were recorded (Table 1). These slopes were substituted in the formula given above for calculating k_b. It was determined that the spring constants of the intact bacteria and the fixed spheroplast were 0.194 and 0.571 nN/nm, respectively. Previously reported spring constants of untreated, intact bacteria range from 0.020 to 0.26 N/m [44,46,47]. The measurements provided in this report are within this range, albeit near the higher end. Variations may be attributed to differences in turgor pressure, protocols for force curve acquisition and physiology of the bacteria. In the case of the fixed spheroplast, the relative rigidity suggested by the spring constant may be due to the effects of the glutaraldehyde as it has been shown to dramatically increase the elastic moduli of mammalian cells [42,43]. On the other hand, when considering the margin of error, the slope measurements

Table 1
Summary of spring constants and indentation distances for bacteria and spheroplasted bacteria

Sample	Cantilever spring constant, k_c (nN/nm)	Slope	Indentation (nm)	Spring constant of bacteria, k_b (nN/nm)
Intact	0.0343 (±0.002)	0.85 (±0.02)	50 (±11.5)	0.194
Fixed spheroplasts	0.036425 (±0.003)	0.94 (±0.06)	20 (±5)	0.571
Untreated spheroplasts	0.0519 (±0.016)	0.97 (±0.05)	160 (±21)	–

on the fixed spheroplasts are only slightly different from the control slope measurements. For the measurement system used here, namely two springs in a series, sensible measurements will be obtained when the two springs have similar spring constants. The similarity of the slopes of the fixed spheroplast to that of the control curve indicates that the surface may be much softer than the value obtained. Therefore, further experiments are required to interpret the data related to the fixed spheroplast. For the untreated spheroplast, the slope is essentially identical to the slope on the control curve. In this case, the spheroplast is much softer than the cantilever and the cantilever does not deflect until after the spheroplast has been indented.

We have chosen to compare the spring constants of the bacteria rather than employ Hertzian models to calculate Young's moduli for comparison as assumptions regarding homogeneous contact surfaces, defined indenter shape, small deformations, infinite sample thickness, and the axisymmetric contact cannot be confirmed in AFM measurements on cells [48–50]. The spring constant is a direct measurement and provides a quantitative basis for comparison within the experimental system and the parameters described in this paper.

4. Conclusions

In this report, spheroplasts of *E. coli* were immobilized on surfaces pretreated with APTES and glutaraldehyde for AFM study. Previously reported methods for immobilizing bacteria are not applicable to spheroplasts because they either rely on adhesion molecules present on intact bacteria surfaces or the trapping of rigid cells in pores. Spheroplasts have neither of these characteristics because the outer wall, which is the source of that rigidity in intact bacteria, is removed. The strategy of chemically cross-linking the spheroplasts to an APTES/Glut substrate described here permits reliable imaging of spheroplasts in liquid.

Imaging spheroplasts with stiffer silicon nitride cantilevers (0.1 nN/nm) is possible, however the softer silicon nitride cantilevers (0.01 nN/nm) resulted in improved height measurements during imaging. Experiments to determine the relative indentation and elasticity of intact bacteria, glutaraldehyde-fixed spheroplasts and untreated spheroplasts revealed that indentation was a significant fraction of the height of the cell. Considering the indentation and the spring constant measurements together, it appears that even the softer silicon nitride cantilevers (0.01 nN/nm) are too stiff to accurately measure the elasticity of the untreated spheroplasts. Due to their morphological similarities, these findings are expected to be applicable to CWD forms of bacteria.

Acknowledgments

This research was sponsored by the Office of Biological and Environmental Research, US Department of Energy. Oak Ridge National Laboratory is managed by UT-Battelle, LLC, for the US Department of Energy under Contract no. DE-AC05-00OR22725.

References

[1] J.W. Costerton, J.M. Ingram, K.J. Cheng, Bacteriol. Rev. 38 (1) (1974) 87.
[2] D.C. Birdsell, E.H. Cota-Robles, J. Bacteriol. 93 (1) (1967) 427.
[3] J. Lederberg, Proc. Natl. Acad. Sci. USA 42 (1956) 574.
[4] J. Lederberg, J.St. Clair, J. Bacteriol. 75 (1957) 143.
[5] E. Ehrenfeld, A.L. Koch, Biochim. Biophys. Acta 169 (1) (1968) 44.
[6] C.M.J. Innes, E.J. Allan, J. Appl. Microbiol. 90 (2001) 301.
[7] M. Elvira-Recuenco, J.W.L. van Vuurde, Microbiol. Res. 158 (4) (2003) 271.
[8] L. Bourgeois, B.L. Beaman, J. Bacteriol. 127 (1) (1976) 584.
[9] Z. Stewart, B. Martinac, J. Dobson, Electro- and Magnetobiol. 19 (1) (2000) 81.
[10] C. Cui, D.O. Smith, J. Adler, J. Membr. Biol. 144 (1) (1995) 31.
[11] B. Tefsen, et al., J. Biol. Chem. 280 (6) (2005) 4504.
[12] M.A. Llamas, et al., J. Bacteriol. 185 (16) (2003) 4707.
[13] H. Abriouel, et al., Appl. Environ. Microbiol. 64 (11) (1998) 4623.
[14] M. Onwuamaegbu, R. Belcher, C. Soare, J. Int. Med. Res. 33 (1) (2005) 1.
[15] G.J. Domingue, H.B. Woody, Clin. Microbiol. Rev. 10 (2) (1997) 320.
[16] V. Beran, et al., Veterinarni Medicina 51 (7) (2006) 365.
[17] V.T. Schuhardt, T.W. Huber, L.M. Pope, J. Bacteriol. 97 (1) (1969) 396.
[18] R.J. Chiodini, et al., J. Clin. Microbiol. 24 (3) (1986) 357.
[19] M. Arnoldi, et al., Appl. Phys. a—Mater. Sci. Process. 66 (1998) S613.
[20] A. Touhami, B. Nysten, Y.F. Dufrene, Langmuir 19 (11) (2003) 4539.
[21] Y.F. Dufrene, Nat. Rev. Microbiol. 2 (6) (2004) 451.
[22] D.P. Allison, P. Hinterdorfer, W.H. Han, Curr. Opin. Biotechnol. 13 (1) (2002) 47.
[23] M. Gad, A. Itoh, A. Ikai, Cell Biol. Int. 21 (11) (1997) 697.
[24] T. Puntheeranurak, et al., J. Cell Sci. 119 (2006) 2960.
[25] G. Pfister, et al., J. Cell Sci. 118 (8) (2005) 1587.
[26] V. Dupres, et al., Nat. Methods 2 (7) (2005) 515.
[27] M.A. Beckmann, et al., Ultramicroscopy 106 (8–9) (2006) 695.
[28] Y.T. Liu, et al., Biotechnol. Bioeng. 93 (2) (2006) 297.
[29] S.E. Cross, et al., Nanotechnology 17 (4) (2006) S1.
[30] A.E. Pelling, et al., Cell Motil. Cytoskeleton 63 (3) (2006) 141.
[31] M.J. Doktycz, et al., Ultramicroscopy 97 (1–4) (2003) 209.
[32] S. Venkataraman, et al., Ultramicroscopy 106 (8–9) (2006) 829.
[33] R. Van Houdt, C.W. Michiels, Res. Microbiol. 156 (5–6) (2005) 626.
[34] J. Pizarro-Cerda, P. Cossart, Cell 124 (4) (2006) 715.
[35] C.J. Sullivan, et al., Ultramicroscopy 105 (1–4) (2005) 96.
[36] H.D. Wang, et al., Biophys. J. 83 (6) (2002) 3619.
[37] J.L. Hutter, J. Bechhoefer, Rev. Sci. Instrum. 64 (7) (1993) 1868.
[38] N.A. Burnham, et al., Nanotechnology 14 (1) (2003) 1.
[39] H.J. Butt, M. Jaschke, Nanotechnology 6 (1) (1995) 1.
[40] S. Kasas, A. Ikai, Biophys. J. 68 (5) (1995) 1678.
[41] J. Kiernan, Microsc. Today 8 (1) (2000) 8.
[42] J.L. Hutter, et al., J. Microsc.—Oxford 219 (2005) 61.
[43] F. Braet, et al., Appl. Phys. a—Mater. Sci. Process. 66 (1998) S575.
[44] M. Arnoldi, et al., Phys. Rev. E 62 (1) (2000) 1034.
[45] X. Li, B.E. Logan, Langmuir 20 (20) (2004) 8817.
[46] S.B. Velegol, B.E. Logan, Langmuir 18 (13) (2002) 5256.
[47] X. Yao, et al., Colloids Surf. B—Biointerfaces 23 (2–3) (2002) 213.
[48] K.D. Costa, A.J. Sim, F.C.P. Yin, J. Biomech. Eng.—Trans. ASME 128 (2) (2006) 176.
[49] W.N. Unertl, J. Vac. Sci. Technol. A 17 (4) (1999) 1779.
[50] A. Alessandrini, P. Facci, Meas. Sci. Technol. 16 (2005) R65.